IJBPAS, September, 2022, 11(9): 4080-4096

ISSN: 2277–4998

International Journal of Biology, Pharmacy and Allied Sciences (IJBPAS)

'A Bridge Between Laboratory and Reader'

www.ijbpas.com

IN VITRO ANTIDIABETIC POTENTIAL OF *Quercus infectoria* GALLS AND *IN SILICO* DOCKING STUDIES OF ISOLATED ROSMARINIC ACID ON α-GLUCOSIDASE ACTIVITY

DSOUZA MR

Department of Biochemistry, Mount Carmel College Autonomous, Bengaluru, India 560052

***Corresponding Author: Myrene R. Dsouza: E Mail: myrene83@gmail.com**

Received 16th Oct. 2021; Revised 20th Nov. 2021; Accepted 20th Jan. 2022; Available online 1st Sept. 2022

https://doi.org/10.31032/IJBPAS/2022/11.9.6353

ABSTRACT

Diabetes mellitus is a fast-growing health concern that affects people all over the world. Despite the availability of synthetic medications, there is always a desire to find herbal formulations owing to their relationship with adverse effects. Traditional healers in India employ *Quercus infectoria* as a folk medicine to reduce inflammation outcomes. The goal of this work is to evaluate the antidiabetic potential of the galls and extract and purify an α-glucosidase inhibitory substance. Antidiabetic potential was evaluated by performing the inhibition of glucose diffusion and inhibition of α-amylase activity. This was followed by *in* silico studies to anticipate the binding interaction of the isolated compound with α-glucosidase using molecular docking studies. To purify the active component, a methanolic extract of *Quercus infectoria* galls was screened for α-glucosidase inhibitory activity and separated into n-butanol, ethyl acetate, and water fractions. HPLC was used to quantify the isolated chemical. AutoDock 4.2.6 was used to conduct the molecular docking investigation. Rosmarinic acid was shown to be the active ingredient in *Q. infectoria* galls that inhibited α-glucosidase with an IC50 of 1.75 µg/ml. In addition, an *in silico* docking research revealed the possibility of rosmarinic acid and αglucosidase binding. The anti-diabetic activity of *Q. infectoria* galls and the isolated component, rosmarinic acid, was confirmed by the findings.

Keywords: α-glucosidase, hyperglycemia, molecular docking, *Quercus infectoria*, rosmarinic acid

INTRODUCTION

The research work on medicinal plants have been phenomenally increasing all over the world. Several developing countries have accepted conventional medical practice as an essential part of their culture. 80% of the population in developing countries rely on traditional medication for their primary health care **[1]**. India contributes considerably to the ever-growing global market. India has about 2.4% of the world's land with 8% of total biodiversity housing 8,000 plant species with documented medicinal use in both treatment of disorders as well as in modern systems of medicines **[2, 3]**. The forest of India is one of the major sources in several aromatic and medicinal plants which are mostly gathered as raw materials to produce drugs. In India, plants have been used for medicinal purposes since Vedic times. The Rig Veda and Atharveda were the first to describe the usage of plants for therapeutic purposes. Most rural populations rely on natural resources such as wild edible plants to satisfy their dietary needs during times of food scarcity **[3]**. At present it is reported that approximately 25% of drugs have been developed from plants with other drugs created from a prototype compound separated from different plant varieties in recent pharmacopoeia **[4]**.

In recent years, diabetes has become a significant cause of death. Diabetes affects 3% of the global population, with the incidence predicted to double to 6.3% by 2025 **[5]**. Authorization, westernisation, and accompanying lifestyle changes, physical inactivity, increased life expectancy at birth, obesity, and perhaps a hereditary susceptibility are the reasons for this predicted increase in prevalence rate **[6]**. It is a metabolic disease marked by hyperglycemia caused by abnormalities in insulin activity and/or secretion. Type 1 diabetes is characterised by a lack of insulin production by pancreatic cells. Type 2 diabetes is linked to obesity and is defined by a growing insulin resistance in the early stages, followed by a decline in pancreatic hormone's capacity to stimulate peripheral glucose clearance and lower hepatic glucose production **[7]**.

Aldose reductase (ALR2; EC: 1.1.1.21), the first rate-limiting enzyme in the polyol pathway, is responsible for forming sorbitol from glucose, utilizing NADPH. Sorbitol dehydrogenase then converts sorbitol to fructose **[8]**. This pathway is usually a secondary route for glucose utilisation, producing less than 3% of total glucose intake. But when blood glucose levels are high, this route becomes more active and can account for up to 30% of the total glucose utilization **[8]**. Several

independent investigations found that ALR2 has a role in diabetic nephropathy, neuropathy, retinopathy, and cataract **[9]**. This pathways credibility as a target for developing diabetic complications prevention methods was reaffirmed. As a result, reducing ALR2 activity looks to be a viable strategy for avoiding diabetes complications. Novel ARI must be developed and evaluated in terms of effectiveness, selectivity, and safety.

Insect galls of *Quercus infectoria* Olivier are the most widely used conventional medicines in Asia for a variety of illnesses. The Allepo oak tree produces these galls as a response to wasps depositing their eggs in the oak bark, which the expanding eggs use for protection and nourishment. Oak galls have long been used to cure dysentery, gonorrhoea, tonsillitis, internal haemorrhages, impetigo, and menorrhagia **[10]**.

MATERIALS AND METHODS

***Preparation of oak gall extract*:** Galls of *Q. infectoria Olivier* were procured from Attar Ayurveda in Jaipur, Rajasthan, for this investigation. Using a pestle and mortar, the dried galls were crushed and then coarsely ground in an electric grinder. Using a rotary shaker, 20 g of gall powder were immersed in 100 ml of the following solvents: water, methanol, ethanol, ethyl acetate, acetone, and hexane, and agitated for 6 h at 200 x g. To remove plant particles, the crude *Q. infectoria* extracts (QIE) were filtered using Whatman filter paper No. 1 in a Buchner funnel, then evaporated at 40°C. By rapid agitation at 45°C, the dry powder was suspended in distilled water to a final concentration of 10% (w/v). The QIE was sterilised and stored at 4 °C in sterile dark vials using a syringe filter of pore size 0.22 µm.

In vitro inhibition of glucose diffusion activity: Using the technique given by Edwards **[11]** the inhibition of glucose uptake by the methanolic QIE was assessed. The process entails filling a sealed dialysis with 1 ml of a solution containing 20 mM glucose and 150 mM NaCl. The amount of glucose that appeared in the external solution was determined. The model utilised in this study consisted of a dialysis tube holding 2 ml of seed extract in 1% CMC and 1 ml of 150 mM NaCl containing 25 ml of 20 mM D-glucose. The dialysis tube was put in a 50 ml beaker containing 45 ml of 150 mM NaCl with each end capped. The tubes were stored at room temperature and shaken on an orbital shaker. At 30, 60, 120, and 180 min, the transfer of glucose into the exterior solution was observed. Metronidazole was utilised as control.

α-amylase inhibitory effect: α-amylase activity was determined by measuring the reducing groups formed by isolated porcine pancreatic α -amylase hydrolyzing soluble

starch. 250 µl of hydromethanolic extract or acarbose at various concentrations (100 - 500 µg/ml) were incubated for 20 min at 37 °C in phosphate buffer (100 mM, pH 6.8) with 500 µl of α -amylase (2 U/ml). After that, 250 µl of 1% starch dissolved in 100 mM phosphate buffer (pH 6.8) was added to the reaction mixture, which was then incubated for 1 hour at 37 °C. The tubes were incubated in a boiling water bath with dinitrosalicylate colour reagent for 10 minutes. The absorbance was measured at 540 nm after cooling. The inhibitory activity on α-amylases were estimated using the following formula:

$$\textbf{Inhibition}\ (\%) = \frac{OD\ of\ control - OD\ of\ sample}{OD\ of\ control} \times 100$$

------- **(Eq. 1)**

α-glucosidase inhibitory effect: 100 µl sample was mixed with 60µl phosphate buffer (0.1 mM, pH 6.8) containing 10 µl α-glucosidase (1 U/ml) or acarbose (0, 500, 1000, 1500, and 2000 µg/ml) and incubated at 37 °C for 10 minutes **[12]**. In 0.1 mM phosphate buffer, 30 µl of 2 mM pNPG (4-Nitrophenyl-D-glucopyranoside) solution was added to start the enzyme reaction. A microplate reader was used to measure absorbance at 405 nm every 15 minutes for 2 hours. The inhibitory action on enzyme activity was calculated from the area under the curve (AUC) for each sample or acarbose and compared with the AUC of the negative control, without sample. Acarbose served as the positive control. The inhibition of enzyme activity was estimated using the formula:

$$\%\ \textbf{Inhibitory effect} = \frac{An - Ai}{An}\ x\ 100$$

where An is the AUC of negative control and Ai is the AUC of solution with inhibitors (sample or the positive control). The inhibitory effects of individual flavonoids and the flavonoids-rich extract were converted into acarbose equivalents to make further analysis easier, and the unit was stated as µg acarbose equivalents/ µg.

Isolation of α-glucosidase inhibitory compound and molecular docking studies

***Extraction and isolation of active compound*:** To generate a hydro-alcoholic solution, dried galls of *Q. infectoria* were extracted three times with methanol followed by the addition of water to make a hydro-alcoholic solution. To eliminate the presence of fatty compounds, the solution was washed with petroleum ether and then concentrated to obtain the dry extract. The dried extract was suspended in distilled water and fractionated into ethylacetate, n-butanol, and water, with ethylacetate, n-butanol, and water being the final products. The butanol fraction was the most active of these fractions, so it was subjected to silica gel column chromatography with increasing polarity – 1:1 petroleum ether-chloroform, 9:1 chloroform – methanol, 4:1 chloroform – methanol, 1:1 chloroform –

methanol, 1:1 chloroform – methanol, and 3:7 chloroform – methanol. Fraction 6 produced the most effective inhibition of -glucosidase. To get the bioactive molecule, this fraction was treated to semi-preparative HPLC (Shimadzu LC20AD with PDA detector). The enriched fraction was used to make a 10 mg/ml solution using 7:3 water and methanol, which was then filtered through a 0.45 µm syringe filter. For analytical and semi preparative separation, 20 µl and 200 µl of the filtrate was injected respectively. The mobile phase was made up of a linear gradient of 1% acetic acid in water and methanol as solvent A and B, respectively. The analytical and semi-preparative flow rates were 1 ml/min and 3 ml/min, respectively. The peaks were collected whilst being eluted from the column and the solvents were evaporated.

Rosmarinic acid (1 mg/ml) standard was diluted to obtain the required test concentrations. The amount of rosmarinic acid present in the various fractions i.e., methanolic extract, n-butanol and the enriched fraction was determined from the calibration curve of the standard solution.

In silico structure prediction of α-glucosidase*:* The protein sequence of α-glucosidase was retrieved from UniProt (www.uniprot.org). It had the Accession Number: P53341. The conserved domain and catalytically important sites were determined using NCBI CDD. Protein molecule structure was retrieved in ".pdb" format. The protein molecule was subjected to removal of all water molecules and addition of only the final stage hydrogen atoms. This was followed by the addition of polar hydrogen atoms and Gasteiger charge. SWISS-MODEL was used to obtain the structural 3D model if the enzyme (https://swissmodel.expasy.org). After this, a homology-based search was done using Protein Data Bank (PDB) repositories. The best suited template with the highest similarity was used to determine biological property and for generating the 3D model. Evaluation of the accuracy of the structure and the Ramachadran plot was confirmed using PROCHECK and ProSA-web **[13]**.

***Preparation of ligand molecule*:** NCBI PubChem database was used to obtain the 3D structure of rosmarinic acid (PubChem CID: 5281792) (https://pubchem.ncbi.nlm.nih.gov/). The ligands were retrieved in 3D structure in ".sdf" format. This was then transformed into ".pdb" format with the help of SMILES Translator (https://cactus.nci.nih.gov/translate/). The converted files were downloaded in ".pdb" format. These ".pdb" files were used to run different tools and softwares.

***Determination of in silico pharmacokinetics, bioactivity, toxicity properties*:** The computational estimation

for rosmarinic acid was accomplished through the online software: Molinspiration (https://www.molinspiration).com/), Pre-ADMET and prediction of ADME/Tox (https://preadmet.bmdrc.kr/), and SwissADME (https://swissadme.ch). Estimation of drug-like parameters such as polar surface area, logP, number of hydrogen bonds, bioactivity score for the most significant drug targets was performed. The assessment of absorption, distribution, metabolism, and excretion is paramount to the understanding of the behaviour of the drug molecule. Parameters such as the ability of the drug to reach the target site in sufficient concentration and its period of bioactivity were assessed by Pre-ADMET. SwissADME, an online tool providing free access to predictive models for pharmacokinetics, physicochemical properties, medical chemistry and drug-likeness. The physicochemical parameters analyzed give a global description of the structure. Toxicity studies were evaluated by *in silico* model using ADMETox prediction software Pentium IV processor. The molecule was drawn and subjected for evaluation of toxicity including neurotoxicity, oncogenicity, immunotoxicity, teratogenicity, etc.

***Preparation through Biovia Discovery Studio Visualizer*:** This software suite was used for analysis and evaluated by removing water molecules, altering missing atoms in incomplete residues, modelling missing loop regions, deleting alternate conformations, and protonating titratable residues. After suitable changes, the crystal structure of the protein was saved in .pdb format. This protein molecule was used for docking.

Preparation of Grid Parameter File: The active site residues used for docking was taken from literature - ASP69, ASP352, GLU277 **[14]**. Grid maps were generated with spacing of 0.375 Å to allow ligand binding. The dimension of the grid was adjusted to 50 × 50 × 50 points. The maps were then analyzed by Auto Grid and the interaction energy at each grid point of the protein was assigned. The interaction energy between every ligand atom and receptor was calculated for the entire binding site. AutoDock Vina was used for docking.

Statistical analysis: Analysis was carried out by using one-way analysis of variance (ANOVA) followed by Dunnett's test. Results are expressed as mean ± SEM. P values < 0.05 were considered significant.

RESULTS AND DISCUSSION

In vitro evaluation of anti-diabetic potential: The human body requires energy to complete essential metabolic operations that keep it alive. Glucose, a basic carbohydrate that works as a key fuel in the generation of energy in brain, muscles and other organs, provides this energy.

Glycoproteins and glycolipids use glucose as a building block. A high quantity of glucose in the body can cause a variety of complications, some of which can be fatal. This, in turn, is maintained by the homeostasis. Diabetes mellitus is characterised by elevated glucose levels and abnormal glucose metabolism. Insulin shortage or resistance causes increased blood glucose, leading in decreased glucose utilisation in insulin-dependent tissues such as the liver and muscle tissues, which require insulin for glucose absorption **[15]**.

In vitro inhibition of glucose diffusion: Glucose uptake transport systems are abundant in animal cells as they perform an important function in transportation of glucose molecules across the cell membrane. The study of glucose absorption by body cells is crucial because it aids in the diagnosis of illnesses and metabolic disorders such as myocardial ischemia, diabetes, and cancer **[15]**. The glucose diffusion tests were performed in order to examine the anti-diabetic effect of QIE. This resulted in varying levels of glucose form the 30^{th} min absorbance up to 180^{th} min absorbance as shown in the **Figure 1**.

From results obtained it is very evident that QIE helps in delaying the glucose diffusion for up to 60 min thereby providing sufficient time for the system to eliminate the glucose and prevent its uptake into the cells of the body. Although a healthy individual requires glucose and individual who is obese, or diabetic may have repercussions. In such cases, QIE can be employed to delay glucose diffusion **(Figure 1)** and help in maintaining glucose-insulin level **[16, 17]**.

α-amylase inhibitory effect: Starch digestion is a multi-stage process in humans. The partial digestion of polymeric substrates by salivary amylase resulted in the formation of shorter oligomers at first. Pancreatic amylases further hydrolyze them in the gut, converting it to maltotriose, maltose, and small malto-oligosaccharides. α-amylase hydrolyzes dietary starch, breaking it down into glucose before absorption. In diabetics, inhibiting α-amylase can lead to a decrease in postprandial hyperglycemia **[17]**. The QIE possesses anti-diabetic activity comparable with the standard, acarbose **(Figure 2)**.

Isolation of α-glucosidase inhibitory compound and molecular docking studies

Quantitative HPLC analysis: The major compound in the enriched fraction after chromatography was found to be rosmarinic acid with the HPLC chromatogram of the compound in the enriched fraction and the isolated rosmarinic acid as depicted **(Figure 2)**. The amount of rosmarinic acid present in 1 g of the enriched fraction was determined from

the calibration curve (y=3333.3x, R^2 = 1.0) (Fig 3) and found to be 453±9.1 mg.

α-glucosidase inhibitory effect: Saccharides present in the food are converted to glucose through the action of α-glucosidase. This contributes to an increase in blood glucose levels. The enriched fraction and rosmarinic acid were found to inhibit α-glucosidase **(Table 1)**, and hence could serve in the postprandial management of diabetes mellitus Type 2. It was also noticed that the percent of inhibition *in vitro* was more pronounced when compared to acarbose.

Docking studies: Molecular docking was performed to understand the interaction between α-glucosidase from *Saccharomyces cerevisiae* and rosmarinic acid. The yeast enzyme, isomaltase **(Figure 4)** was chosen as the experimental model due to its similarity in substrate specificity, inhibitor sensitivity and pH optima **[18]** when compared to human glucosidase and has been used to understand the mechanism of action of human glucosidase. Maximum homology was obtained for isomaltase 3AJ7. Homology study was done as the 3D structure of yeast α-glucosidase was not available. MAL12 (*S. cerevisiae* isomaltase (PDB ID: 3AJ7, Chain A) was used as the template for building the 3D structure of yeast α-glucosidase as it possessed 99% query coverage and 72% similarity when compared to the enzyme **(Figure 5)**. Evaluation of the accuracy of the structure and the Ramachadran plot was confirmed using PROCHECK **(Figure 5)**. The Ramachandran plot indicated that 88.8% of residues were discovered in the most favoured areas, 10.6% were found in other allowed regions, 0.4% were seen in generously allowed regions, and just 0.2% occurred in the disallowed regions.

Preparation of ligand molecule: NCBI PubChem database (https://pubchem.ncbi.nlm.nih.gov/) was used to obtain the 3D structure of rosmarinic acid (PubChem CID: 5281792). The ligands were retrieved in 3D structure in ".sdf" format. This was then converted into ".pdb" format through online SMILES Translator (https://cactus.nci.nih.gov/translate/) (Berman *et al*., 2000). The converted files were downloaded in ".pdb" format. These ".pdb" files were used to run different tools and software's **(Figure 6)**.

Determination of *in silico* pharmacokinetics, bioactivity, toxicity properties: The computational calculation for rosmarinic acid was executed through online software: Molinspiration (https://www.molinspiration).com/), Pre-ADMET and prediction of ADME/Tox (https://preadmet.bmdrc.kr/), and SwissADME (https://swissadme.ch). Rosmarinic acid **(Figure 6)** was analyzed for pharmacokinetic properties and drug

likeness following the Lipinski's rule of five **(Figure 7)** The molecular weight of the selected drug falls in the appropriate range of ≤ 500) Da. This is an important parameter to easy absorption, diffusion and transportation in comparison to high molecular weight compounds. The MLogP (octanol/ water partition coefficient), used to determine lipophilic efficiency was also found to be within permissible range as per Lipinski's rule. The logP value of the octanol-water partition coefficient is critical in rational drug design and QSAR investigations. Calculating the logP value is needed to determine the hydrophobicity of a drug candidate as hydrophobicity affects the drugs distribution throughout the body. TPSA (Topological Polar Surface Area) is a metric that measures the polarity of substances and is used to assess drug transport abilities. Molecular volume evaluates a transport capability of the compound in areas like penetration of blood-brain barrier. The flexibility is determined by the amount of rotatable bonds, which leads to strong binding affinity with the binding pocket.

The bioactivity score provides evidence of the binding of the drug molecule. This parameter is important for the development of drug possessing increased binding selectivity and less side effects. Bioactivity score greater than 0.00 indicates that the drug has significant biological activity, while scores of 0.5 - 0.00 and less than -0.50 is said to be moderately active and inactive respectively **[19]**. Rosmarinic was found to have biological activity as inhibitor of proteases and as a nuclear receptor ligand and GPCR ligand **(Figure 9)**.

The goal of medicinal chemistry findings is to help drug discovery activities on a daily basis. As a result, the SwissADME programme provides two complimentary pattern recognition filters (PAINS and Brenk) that permit the detection of possibly challenging segments in the molecules under investigation. The programme generates warnings if any of the listed fragments are detected in the molecule under investigation. 1 alert for catechol was produced in PAINS and 2 alerts corresponding to catechol and micheal_acceptor_1 was generated by Brenk **(Figure 10)**. In terms of these metrics, rosmarinic acid showed a low gastrointestinal absorption ability, which is consistent with the basicity of the molecule, as well as appropriate skin permeability values of -6.82 cm/s. Rosmarinic acid may act as a P-glycoprotein (P-gp) inhibitor rather than a substrate in terms of absorption. This is significant because P-glycoprotein is an efflux transporter that acts as an absorption barrier in a variety of compartments, including the

gastrointestinal membranes and lumen wall, as well as the membranes of the brain. To avoid development failure, most pharmaceutical firms have developed a series of *in vitro* ADME/Tox screens with the goal of eliminating compounds in the initial phase of discovery that could probably fail later. Even while early stage in vitro ADME decreases the likelihood of development stage failure, however this process is still laborious and expensive **(Table 3)**. Rosmarinic acid is a non-mutagen when tested using the Ames test and is generally nontoxic. It is not probable to toxicity except for hERG inhibition.

The docking of rosmarinic acid with protein target was studied using AutoDock Vina and Biovia Discovery Studio Client 2020. Software indicated that the ligand possessed minimum binding energy for active site of -7.72 kcal/mol. The binding free energy (ΔG) between the ligand and receptor is -19.14 kcal/mol indicating inhibition of α- glucosidase by rosmarinic acid **(Figure 11)**.

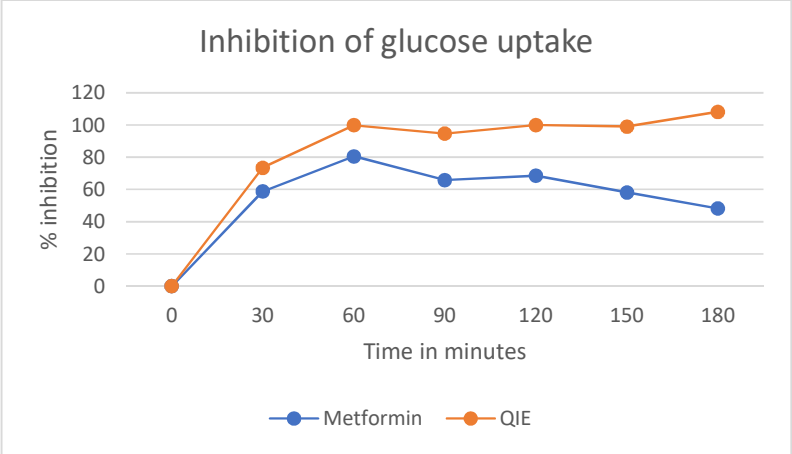

Figure 1: Graphical representation of the effect of QIE on the movement of glucose out of dialysis tube for every 30 min for 180 min

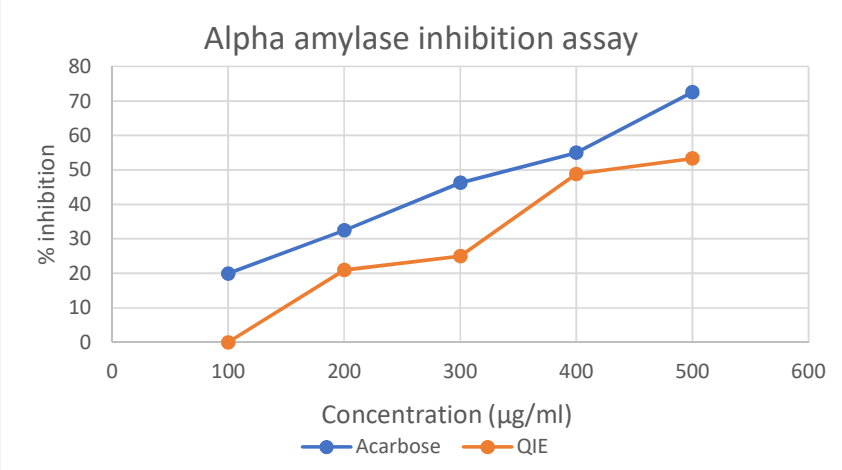

Figure 2: Inhibition of α-amylase by QIE in comparison to the standard drug Acarbose

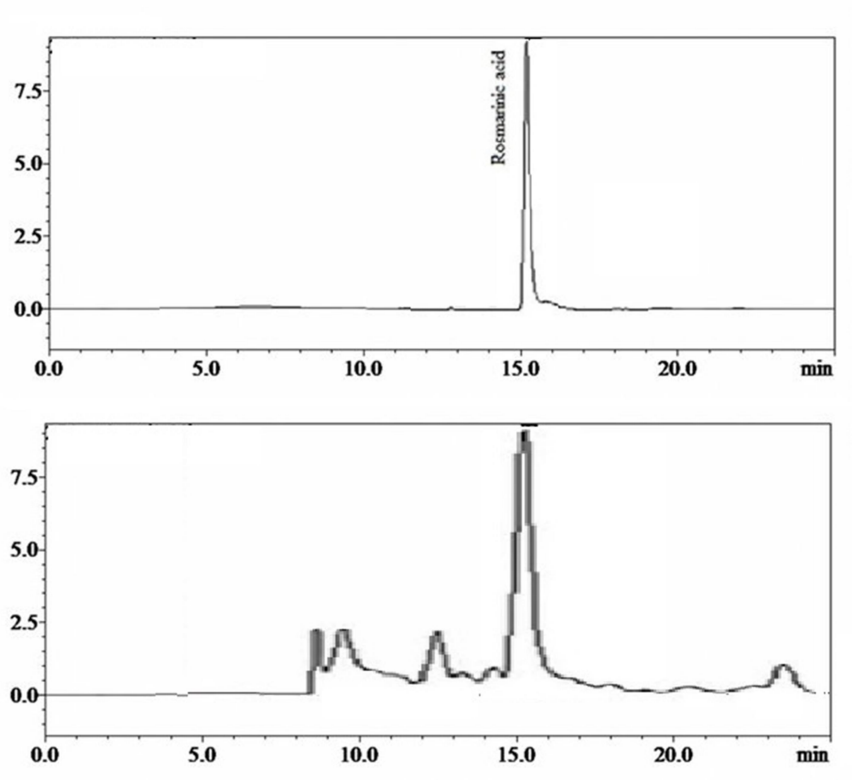

Figure 3: H PLC chromatogram of standard rosmarinic acid (a) and enriched fraction no 6, illustrating the peak of rosmarinic acid against the retention time

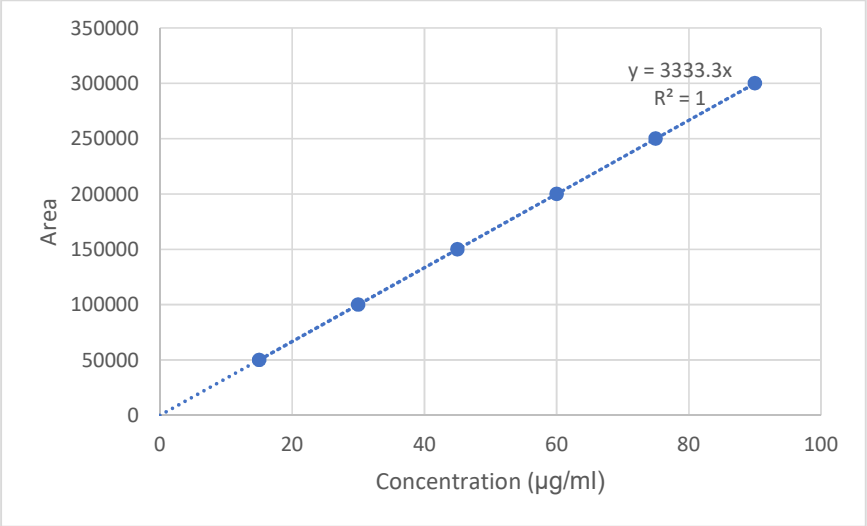

Figure 4: Calibration curve of standard rosmarinic acid as obtained from the HPLC chromatogram

Table 1: IC50 of the analyzed samples on the enzyme α-glucosidase

Samples	IC50 (µg/ml)
Acarbose	81.9 ± 4.6
Methanolic extract	1.75 ± 0.31
Water fraction	Absence of inhibition up to 500 µg/ml
Sub fraction 6	0.72 ± 0.04
Rosmarinic acid	0.27 ± 0.05

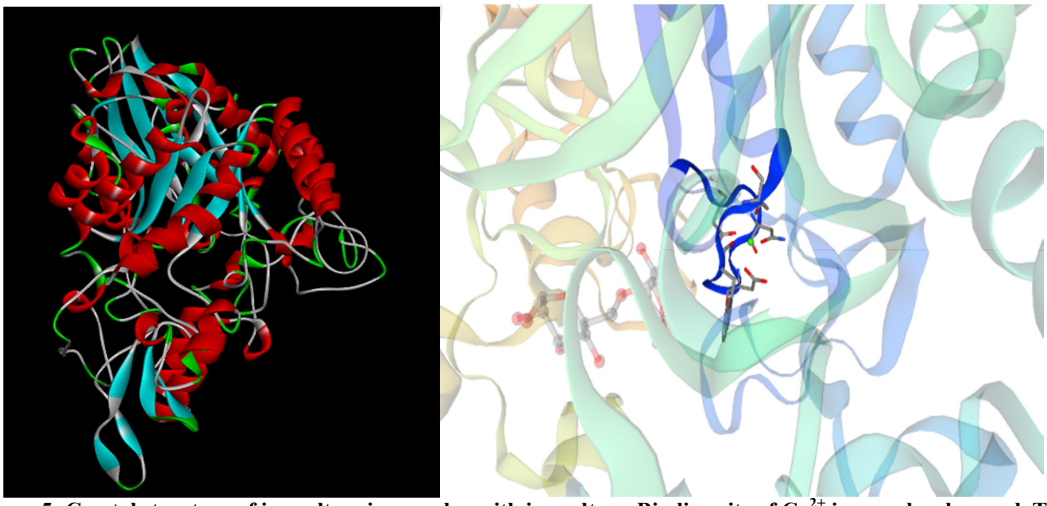

Figure 5: Crystal structure of isomaltase in complex with isomaltose. Binding site of Ca^{2+} ion can be observed. This 3D model was generated for the highest similarity to determine biological property

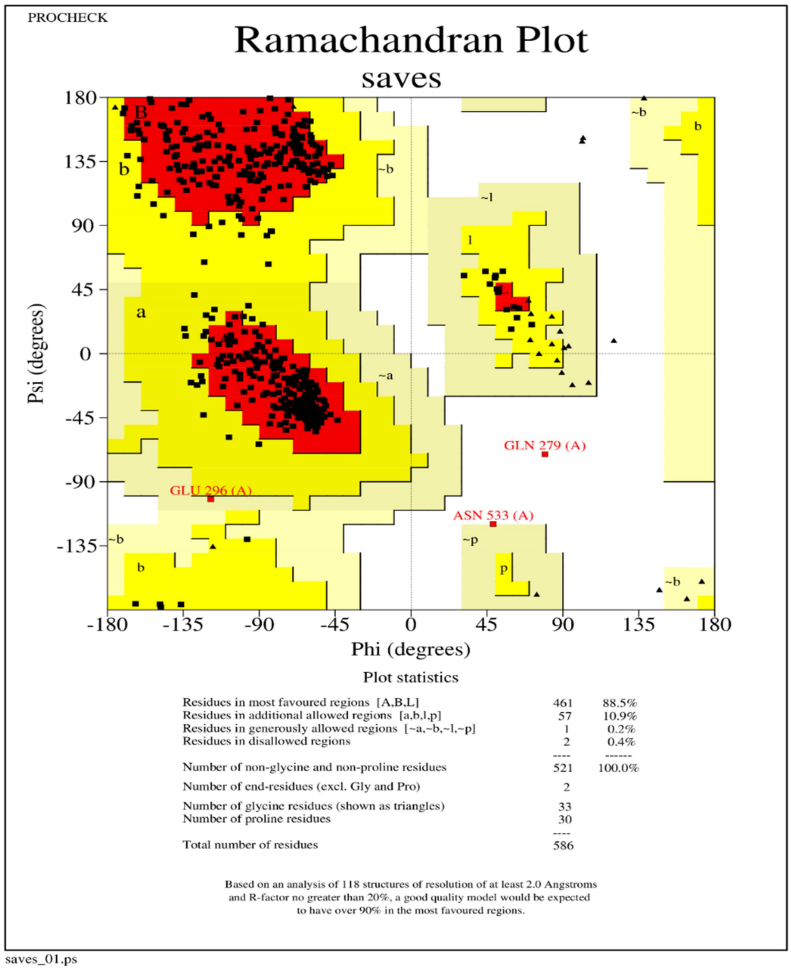

Figure 6: Confirmation of accuracy of the structure by the Ramachandran plot using PROCHECK

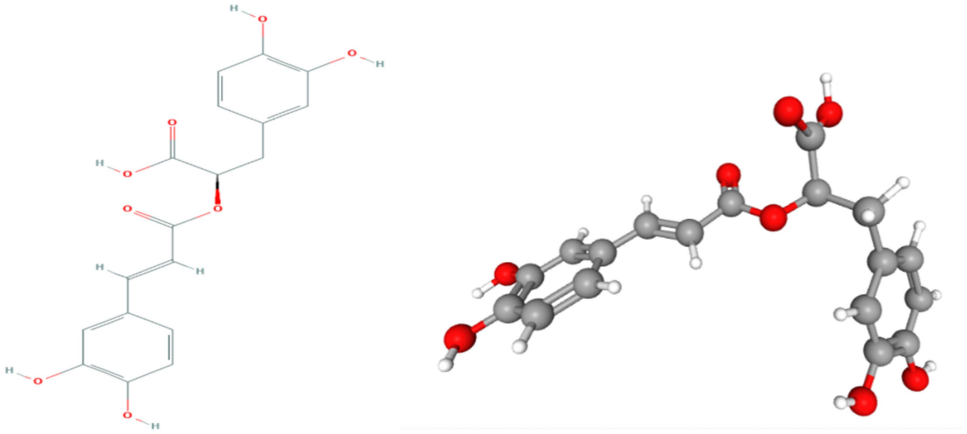

Figure 7: Structure of Rosmarinic acid; 2D (A) and 3D (B)

molinspiration

originalSMILES C1=CC(=C(C=C1C[C@H](C(=O)O)OC(=O)/C=C/C2=CC(=C(C=C2)O)O)O)O
miSMILES: C1=CC(=C(C=C1C[C@H](C(=O)O)OC(=O)/C=C/C2=CC(=C(C=C2)O)O)O)O

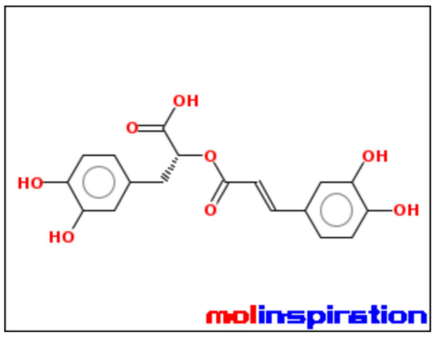

Molinspiration property engine v2018.10

miLogP	1.63
TPSA	144.52
natoms	26
MW	360.32
nON	8
nOHNH	5
nviolations	0
nrotb	7
volume	303.54

Figure 8: Pharmacokinetic parameters of rosmarinic acid

molinspiration

originalSMILES C1=CC(=C(C=C1C[C@H](C(=O)O)OC(=O)/C=C/C2=CC(=C(C=C2)O)O)O)O
miSMILES: C1=CC(=C(C=C1C[C@H](C(=O)O)OC(=O)/C=C/C2=CC(=C(C=C2)O)O)O)O

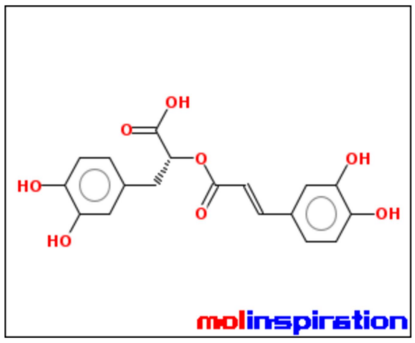

Molinspiration bioactivity score v2018.03

GPCR ligand	0.17
Ion channel modulator	-0.08
Kinase inhibitor	-0.18
Nuclear receptor ligand	0.57
Protease inhibitor	0.15
Enzyme inhibitor	0.24

Get data as text (for copy / paste).

Get 3D geometry BETA

Figure 9: Bioactivity scores of rosmarinic acid

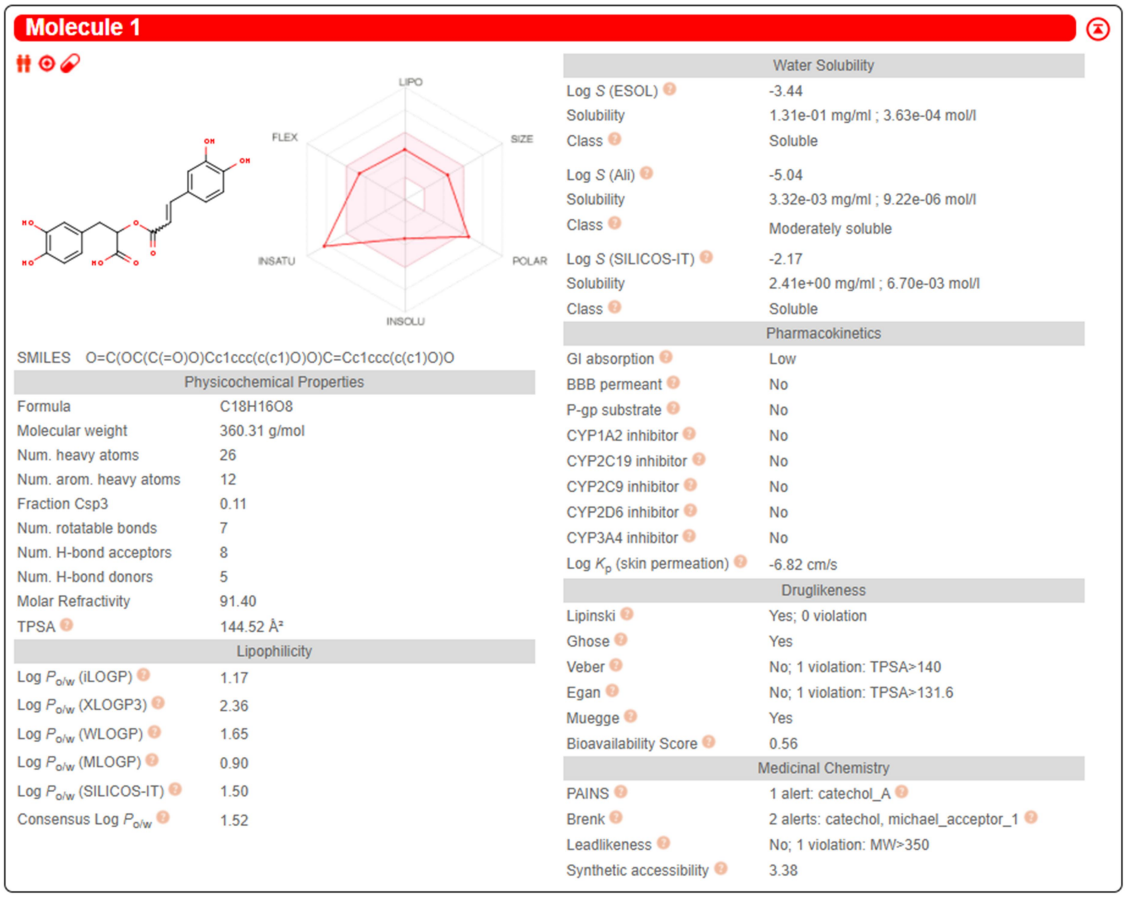

Figure 10: Drug likeness – PreADMET prediction

Table 3: Toxicity profile of rosmarinic acid

Model ID	Value	Model ID	Value
Algae_at	0.0102013	Medaka_at	0.0157562
Ames_test	Non-mutagen	Minnow_at	0.0242226
Carcino_mouse	Negative	TA100_10RLI	Negative
Carcino_rat	Positive	TA100_NA	Negative
Daphania_at	0.0917228	TA1535_10RLI	Negative
hERG_inhibition	Medium risk	TA1535_NA	Negative

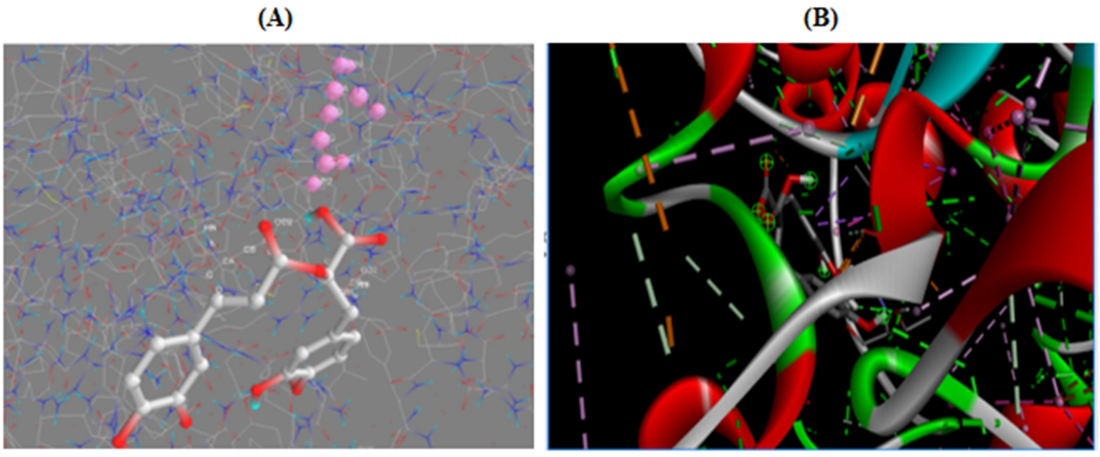

Figure 11: Docking result of rosmarinic acid with the active site residues (A), Ligand interaction at active site showing protein groups, interface groups and interacting receptors (B)

CONCLUSION

The anti-diabetic potential of galls of *Quercus infectoria* and the primary active ingredient rosmarinic acid has been described for the first time. Furthermore, the *in silico* binding investigation of rosmarinic acid with α-glucosidase enzyme from *S. cerevisiae* was described in this work.

ACKNOWLEDGMENTS: The author is grateful to Mount Carmel College, Autonomous,

Bengaluru, Karnataka, India, for the provision of funding and facilities needed for conducting this project.

REFERENCES

[1] Ekor, M. (2014). The growing use of herbal medicines: issues relating to adverse reactions and challenges in monitoring safety. Frontiers in pharmacology, 4, 177.

[2] Kala, C. P., Dhyani, P. P., & Sajwan, B. S. (2006). Developing the medicinal plants sector in northern India: challenges and opportunities. Journal of Ethnobiology and Ethnomedicine, 2, 32.

[3] Gowthami, R., Sharma, N., Pandey, R., & Agrawal, A. (2021). Status and consolidated list of threatened medicinal plants of India. Genetic resources and crop evolution, 1–29. Advance online publication.

[4] Bhatia, H., Sharma, Y.P., Manhas, R.K. et al., (2018) Traditionally used wild edible plants of district Udhampur, J&K, India. J Ethnobiology Ethnomedicine, 14, 73.

[5] Saeedi, P., Petersohn, I., Salpea, P., Malanda, B., Karuranga, S., Unwin, N., Colagiuri, S., Guariguata, L., Motala, A. A., Ogurtsova, K., Shaw, J. E., Bright, D., Williams, R., & IDF Diabetes Atlas Committee (2019). Global and regional diabetes prevalence estimates for 2019 and projections for 2030 and 2045: Results from the International Diabetes Federation Diabetes Atlas, 9th edition. Diabetes research and clinical practice, 157, 107843.

[6] Mobasseri, M., Shirmohammadi, M., Amiri, T., Vahed, N., Hosseini Fard, H., & Ghojazadeh, M. (2020). Prevalence and incidence of type 1 diabetes in the world: a systematic review and meta-analysis. Health promotion perspectives, 10(2), 98–115.

[7] Sharabi, K., Tavares, C. D., Rines, A. K., & Puigserver, P. (2015). Molecular pathophysiology of hepatic glucose production. Molecular aspects of medicine, 46, 21–33.

[8] Yan L. J. (2018). Redox imbalance stress in diabetes mellitus: Role of the polyol pathway. Animal models and experimental medicine, 1(1), 7–13.

[9] Guzman, A., Guerrero, O.R. (2005). Inhibition of aldose reductase by herbs extracts and natural substances and their role in prevention of cataracts. Revista Cubana de Plantas Medicinales, 10, 3-4.

[10] Warrier, P.K., Nambiar, V.P.K., Ramankutty, C., (1995) Indian Medicinal Plants, Orient Longman, Madras, India, 4th edition.

[11] Edwards, C. A., Blackburn, N. A., Craigen, L., Davison, P., Tomlin, J., Sugden, K., Johnson, I. T., & Read, N. W. (1987). Viscosity of food gums determined in vitro related to their hypoglycemic actions. The American journal of clinical nutrition, 46(1), 72–77.

[12] Zhang, H., Wang, G., Beta, T., & Dong, J. (2015). Inhibitory properties of aqueous ethanol extracts of propolis on alpha-glucosidase. *Evidence-based complementary and alternative medicine: eCAM*, *2015*, 587383.

[13] Wiederstein, M., & Sippl, M. J. (2007). ProSA-web: interactive web service for the recognition of errors in three-dimensional structures of proteins. *Nucleic acids research*, *35*(Web Server issue), W407–W410.

[14] Yamamoto, K., Miyake, H., Kusunoki, M., & Osaki, S. (2010). Crystal structures of isomaltase from Saccharomyces cerevisiae and in complex with its competitive inhibitor maltose. *The FEBS journal*, *277*(20), 4205–4214.

[15] Bordia, A., Verma, S. K., & Srivastava, K. C. (1997). Effect of ginger (Zingiber officinale Rosc.) and fenugreek (Trigonella foenumgraecum L.) on blood lipids, blood sugar and platelet aggregation in patients with coronary artery disease. *Prostaglandins, leukotrienes, and essential fatty acids*, *56*(5), 379–384.

[16] Ningthoujam, S., Dsouza, M.R., and Alisha (2018) Pharmacological evaluation of Parkia speciosa Hassk. for antioxidant, anti-inflammatory, anti-diabetic and antimicrobial activities in vitro, International Journal of Lifesciences, Special Issue, A11: 49-59

[17] Hana, C.D., Rufina K., Dsouza, R. D., (2019) Diosgenin from Dioscorea Alata: Extraction and Potential Effects on Enzymes Related to Metabolic Syndrome. International Journal of Pharmacy and Biological Sciences, 9: 177-185.

[18] Brito-Arias, M., Ramírez-Hernández, P.L., García-Barrera,E.C., Perez-Venegas,M., Montiel-Valenciana, C. and Rodríguez-Pascual, L.P. (2018)

Synthesis, α-Glucosidase Enzymatic Inhibition and Docking Studies of some Fused Heterocycles. Chemical & Pharmaceutical Research, 1(1), 1-6.

[19] Verma A., (2012) Lead finding from *Phyllanthus debelis* with hepatoprotective potentials, Asian Pacific J. Trop. Biomed. 3, S1735-S1737.